Non-coding RNA Research 4 (2019) 141–154

Contents lists available at ScienceDirect

Non-coding RNA Research

journal homepage: http://www.keaipublishing.com/ncrna

Identification of novel microRNAs and their targets in Chlorophytum borivilianum by small RNA and degradome sequencing

Monika Kajal, Nishant Kaushal, Ravneet kaur, Kashmir Singh*

Department of Biotechnology, Panjab University, BMS Block-I, Sector 25, Chandigarh, 160014, India

ARTICLE INFO

Keywords:
Degradome
Chlorophytum borivilianum
microRNAs
Illumina sequencing
SRA

ABSTARCT

Plant specific miRNAs (Novel miRNAs) are well known to perform distinctive functions in biological processes. Identification of new miRNAs is necessary to understand their gene regulation. Degradome provides an opportunity to explore the miRNA functions by comparing the miRNA population and their degraded products. In the present study, Small RNA sequencing data was used to identify novel miRNAs. Further, degradome sequencing was carried out to identify miRNAs targets in the plant, *Chlorophytum borivilianum*. The present study supplemented 40 more novel miRNAs correlating degradome data with smallRNAome. Novel miRNAs, complementary to mRNA partial sequences obtained from degradome sequencing were actually targeting the later. A big pool of miRNA was established by using *Oryza sativa, Arabidopsis thaliana, Populus trichocarpa, Ricinus communis,* and *Vitis vinifera* genomic data. Targets were identified for novel miRNAs and total 109 targets were predicted. BLAST2GO analysis elaborate about localization of novel miRNAs' targets and their corresponding KEGG (Kyoto Encyclopedia for Genes and Genomes) pathways. Identified targets were annotated and were found to be involved in significant biological processes like Nitrogen metabolism, Pyruvate metabolism, Citrate cycle (TCA cycle), photosynthesis, and Glycolysis/Gluconeogenesis. The present study provides an overall view of the miRNA regulation in multiple metabolic pathways that are involved in plant growth, pathogen resistance and secondary metabolism of *C. borivilianum*.

1. Introduction

C. borivilianum Santapau & Fernandes is an important perennial herb of liliaceae family. Under cultivated condition it is used as an annual crop. In the recent time good market demand has been observed for the *C. borivilianum* roots. This is because root powder possess.

Numerous pharmaceutical properties such as immunomodulatory [1], anti-diabetic [2], pendiculatory [3], and androgenic [4] etc. The dried roots of *C. borivilianum* (also known as "Safed musli") is an Indian herb and majorly used for the curing rheumatism and helpful in enhancing the immunity. Now a days a number of pharmaceutical industries are using the root extract of *C. borivilianum* in their formulations for example Dabur, India; Emami Limited, India; Patanjali, India; Nutri Herbs Pvt. Ltd, Malaysia etc. In the year 2009 FAO (Food and Agriculture Organization of the United Nations) reported root tuber of *C. borivilianum* as widely traded NTFPs (Non-Timber Forest Product) from India. So, its rapid exploitation resulted in its extinction. And then in 2015, this plant was included in the Red data list of IUCN as critically endangered species and its population trend is still decreasing due to commercial exploitation [5]. To better utilise the unabridged potential of this substantial herb, it is crucial to know about the molecular aspects of its metabolic networks. Our previous studies on functional genomics of saponins biosynthesis in *C. borivilianum* had identified all the genes involved in saponins biosynthesis using degenerate primers approach [6], suppression subtractive hybridization [7] and by transcriptome sequencing using Illumina HiSeq sequencing platform [8,9].

microRNAs (miRNAs) are known as molecular non-coding regulators of length 18–24 nt. From 5′ end of miRNAs, 2 to 8 nucleotide region is known as "seed" sequence. The seed sequence plays a vital role in the identification and binding to exact target mRNA [10]. The

Abbreviations: AGO, Argonaute; BLAST, Basic local Alignment Search Tool; BP, Biological Process; CC, Cellular Component; FAO, Food and Agriculture Organization of the United Nations; GO, Gene Ontology; IL, Interleukin; iNOS, Inducible Nitric Oxide Synthase; KEGG, Kyoto Encyclopedia of Genes and Genomes; MCF-7, PC3, HCT-116, Types of cell lines; MEP, 2-*C*-methyl-Derythritol-4-phosphate pathway; MF, Molecular Function; MFEs, Minimum Fold Energies; mgmL−1, milligram per millilitre; MTT, 3-(4,5-dimethylthiazol-2-yl)-2,5-diphenyl tetrazolium bromide; MVA, Mevalonic Acid Pathway; nt, nucleotide; RdDM, RNA-directed DNA methylation; SRA, Sequencing Read Archieve; TNF, Tumor Necrosis Factor

* Corresponding author.
E-mail addresses: kashmirbio@pu.ac.in, kashmir123@gmail.com (K. Singh).

https://doi.org/10.1016/j.ncrna.2019.11.004
Received 10 October 2019; Received in revised form 20 November 2019; Accepted 21 November 2019
Available online 25 November 2019

cleavage site occurs between 9 and 11 nt from the 5′ end of the miRNA, and the perfect complementarity at seed region is needed for the mRNA degradation. Fascinatingly, loss of even a single base-pairing in seed region can results into translational repression [11]. Translational repression predominantly occur in animals while plant miRNAs mainly target mRNA by cleavage [12]. This suggest the high complementarity of miRNA with their target mRNA in plants. Due to high degree of miRNA-mRNA complementarity without a single mismatch, chances of occurrence of cleavage are more than translational repression [13]. RNaseH activity of the PIWI domain of AGO proteins is responsible for target cleavage and it does require the 3′ deadenylation or 5' decapping before cleaving as in case of exonuclease [14,15]. mRNA cleavage occurs in plants more commonly because of perfect complementarity between miRNAs and their targets. The improvement in molecular biology verified the contribution of miRNAs in regulating plant metabolic processes with high specificity at the transcriptional and post-transcriptional level. These can be used as a potential molecules to improve plant productivity [16].

In our previous study, we identified 442 known miRNAs belonging to 47 miRNA families and 5 novel miRNAs through small RNA sequencing of young leaf tissue of *C. borivilianum*. We studied the co-relation of miRNAs with the genes involved in the saponin biosynthetic pathway [17]. In the present study we tried to supplement the already present list of *C. borivilianum* miRNAs by digging deep in the RNA population. The combined analysis of the small RNA and degradome sequencing (Parallel analysis of RNA ends) data confirmed the miRNA-mRNA interaction. Degradome profiling confirm the miRNA-mRNA interaction and helps in identification of novel targets. It is proven by multiple studies that miRNA cleavage site lies mostly between 10th and 11th nucleotide from the 5' end of miRNA. After this cleavage, upstream fragment of the target gets degrade and the downstream fragment remains stable. This uncapped, polyadenylated mRNAs can be sequenced to know the exact targeted position [18–20]. So the degradome sequencing will presented the improved picture of the miRNA regulation of various metabolic pathways in this plant. The degradation products of miRNAs can help in identifying the particular molecular pathways extensively regulated by miRNAs. In the present study, starting from a wide approach for identification of novel miRNAs as the genome of the particular plant is not available, we found total 2144 novel miRNAs. This provided a wide spectrum of all the possible miRNAs present in *C. borivilianum*. Further degradome sequencing revealed total 109 probable targets of the identified novel miRNAs. This helped us to recognise the functional aspect of the miRNAs. And on the basis of above analysis we confirmed 40 new novel miRNAs apart from 5 previously reported novel miRNAs.

2. Results

Processed data accessible from our previous study was used for further exploring the novel miRNA pool of *C. borivilianum*. Filtered sequences left after known miRNAs identification were utilised here for identification of novel miRNA.

2.1. Identification of novel miRNAs

Genome of *C. borivilianum* is not known yet, thus genomic data of *A. thaliana, O. sativa, V. vinifera, P. trichocarpa,* and *R. communis* was used for novel miRNAs identification. miRDeep2 (version 2.0.0.7) was used for the prediction of novel miRNAs. From this alignment, we found total 87, 714, 537, 313, 493 novel miRNAs correspond to the *A. thaliana, O. sativa, P. trichocarpa, R. communis,* and *V. vinifera* respectively. This summed up to total novel miRNAs i.e. 2144 pointedly high abundance of miRNAs in *C. borivilianum*. Maximum alignment of novel miRNA population was with *O. sativa*. Among all the selected plant species only *O. sativa* is monocot. This observation of abundant novel miRNAs similarity with *O. sativa*, suggested the significant difference at the level of molecular gene regulation by miRNAs in monocots and dicots. Details of all novel miRNAs from all reference genomes are mentioned in Supplementary Tables 1, 2, 3, 4, 5 respectively. Certainty of all identified miRNAs depends on functions, they are supposed to perform in the actual system of plant. This led us to dogged up further for their actual targets.

2.2. Identification of targets for novel miRNAs

In our previous study we tried to find targets of miRNAs on the basis of transcriptome data of leaf and root tissue [17]. Further to confirm the identified miRNA-mRNA pairs and to minimize the false positives due to the bioinformatics tools, we conducted degradome sequencing analysis. Degradome sequencing of the miRNA-cleaved mRNAs was executed to know the biological functions of identified miRNAs in *C. borivilianum*. For better results we used RNA with the RIN value ≥ 7 for the degradome library preparation. Raw data was processed and the low-quality sequences were discarded altogether, a total of 14,726,700 reads were used to detect miRNA cleavage site. From Cleaveland4 pipeline, 28 novel miRNAs were shown to target 61 transcripts from leaf

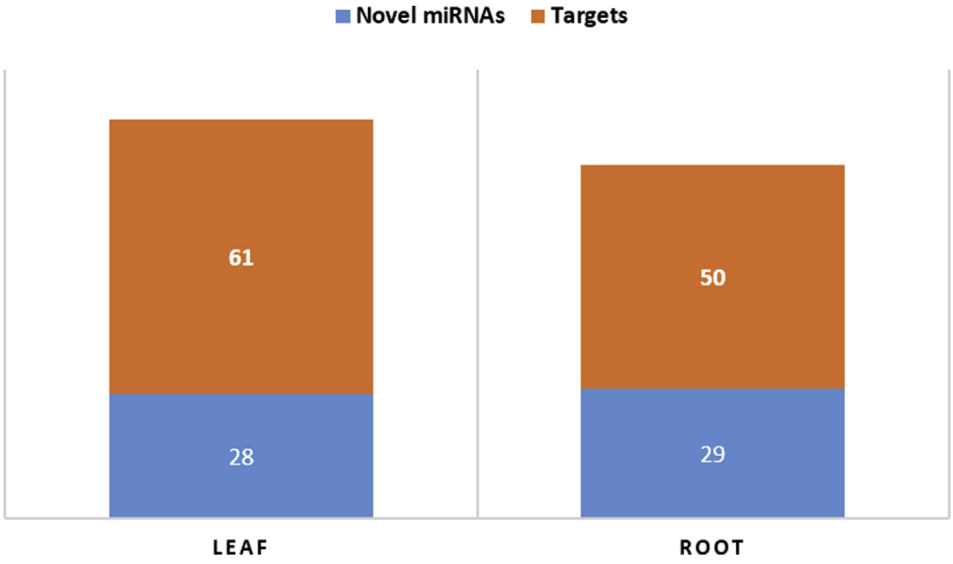

Fig. 1. Representation of abundance of novel miRNA targets from both leaf and root of *C. borivilianum.*

Table 1
Significant targets identified for the novel miRNAs from root transcriptome by parallel analysis of RNA ends. SiteID: Unique name in the format of [Transcript ID]:[Splice Site], Query: miRNA name, Transcript: Transcript Name, TStart: Alignment start position with transcript [One based], TStop: Alignment end position with transcript [One based], TSlice: Splice site in the transcript [One based], MFE perfect: Minimum free energy for perfectly matched site, MFE site: Minimum free energy for alignment in question, MFE ratio: MFE site/MFE perfect, AllenScore: Penalty score calculated per Allen et al. (2005) Cell, 121:207–221, Sequence: Aligned sequence, Degradome Category:0–4, Degradome *P*-val: p-value for degradome hit.

Novel miRNA	Transcript ID	Transcript Annotation	T Start	T Stop	T Slice	MFE Perfect	MFE site	MFE ratio	Allen Score	Degradome Category	Degradome Pval
cbo-miR6	NODE_127333	peroxisomal(S)-2-hydroxy-acid oxidase	839	857	848	−27.1	−18	0.6642066	9	3	0.5762466
cbo-miR7	NODE_169749	probable galacturonosyltransferase 13	20	37	28	−32.9	−21.6	0.656535	4	2	0.5583392
cbo-miR8	NODE_16375	eukaryotic translation initiation factor 3 subunit G	307	326	317	−39.5	−26.2	0.6632911	14	3	0.5182187
cbo-miR9	NODE_3011	pyrophosphate-energized vacuolar membrane proton pump	47	66	58	−35	−22.9	0.6542857	6	3	0.8391801
cbo-miR11	NODE_159572	kinase APK1B, chloroplast precursor	93	107	100	−31.3	−20.5	0.6549521	6	4	0.8002364
cbo-miR11	NODE_62699	cytochrome P450 CYP736A12	10	32	23	−31.3	−21.1	0.6741214	9.5	4	0.6475168
cbo-miR13	NODE_12903	GDP-mannose 3,5-epimerase 1	156	174	165	−37.9	−24.9	0.6569921	7.5	3	0.5731716
cbo-miR15	NODE_28267	V-type proton ATPase 16 kDa proteolipid subunit-like	38	71	48	−43.5	−28.6	0.6574713	34	3	0.5094309
cbo-miR17	NODE_84512	3-ketoacyl-CoA synthase 12-like	219	241	232	−44.3	−31	0.6997743	7	3	0.7351459
cbo-miR19	NODE_160962	probable NADH dehydrogenase [ubiquinone] 1 alpha subcomplex subunit 5, mitochondrial	480	503	489	−34	−22.7	0.6676471	17	4	0.8651497
cbo-miR19	NODE_168980	protein ENHANCED DISEASE RESISTANCE 2-like isoform X1	102	118	111	−34	−22.3	0.6558824	9	4	0.9351247
cbo-miR20	NODE_159279	beta-galactosidase	203	223	213	−35.2	−22.9	0.6505682	8.5	4	0.8041774
cbo-miR20	NODE_53852	UDP-xylose transporter 3 isoform X1	127	146	136	−35.2	−23.2	0.6590909	7	4	0.7288549
cbo-miR21	NODE_135485	transketolase, chloroplastic	90	106	97	−35.4	−23.3	0.6581921	5.5	4	0.8143106
cbo-miR21	NODE_5941	Alpha amylase	61	78	69	−35.4	−23.4	0.6610169	9.5	4	0.8015588
cbo-miR22	NODE_113332	pheophytinase, chloroplastic	155	178	165	−34.9	−24.2	0.6934097	15	4	0.5325574
cbo-miR23	NODE_52274	alanine–glyoxylate aminotransferase 2 homolog 1, mitochondrial	235	254	245	−32.6	−21.6	0.6625767	7.5	4	0.5215639
cbo-miR24	NODE_68726	ferredoxin–NADP reductase, leaf isozyme, chloroplastic	95	114	105	−33.8	−23.5	0.6952663	5.5	3	0.9535455
cbo-miR25	NODE_189501	transcription factor MYB1R1	182	201	192	−30.2	−19.7	0.6523179	11	4	0.5231501
cbo-miR26	NODE_106136	phytoene desaturase	1010	1030	1021	−29	−19.2	0.662069	9.5	2	0.7984963
cbo-miR29	NODE_15305	cysteine proteinase 1-like	168	185	176	−29.1	−19.9	0.6838488	7	2	0.5121175
cbo-miR30	NODE_161012	dynein light chain 1, cytoplasmic	240	259	248	−29	−19.5	0.6724138	9.5	3	0.8365424
cbo-miR30	NODE_80304	thioredoxin H2-2	204	221	212	−29	−20	0.6896552	8.5	4	0.5130147
cbo-miR31	NODE_118499	zinc finger CCCH domain-containing protein 32	348	367	358	−33.8	−22.3	0.6597633	5	3	0.9945255
cbo-miR31	NODE_146239	ABC transporter F family member 5	707	729	719	−33.8	−24.5	0.7248521	8.5	4	0.673437
cbo-miR32	NODE_171312	Phosphoethanolamine *N*-methyltransferase 1	7	25	16	−32.3	−22	0.6811146	8.5	4	0.7884003
cbo-miR32	NODE_5565	probable aquaporin PIP2-5	124	144	135	−32.3	−22.7	0.7027864	9.5	3	0.8168269
cbo-miR33	NODE_153391	acyl-coenzyme A oxidase 4, peroxisomal	1082	1100	1091	−22.5	−15.2	0.6755556	11	3	0.8151639
cbo-miR33	NODE_159321	alpha-1,3/1,6-mannosyltransferase ALG2-like	1060	1078	1069	−22.5	−15.1	0.6711111	11.5	2	0.6361594
cbo-miR33	NODE_57190	ferredoxin-NADP + reductase	60	78	69	−22.5	−14.8	0.6577778	10	4	0.7633698
cbo-miR36	NODE_115533	probable serine/threonine-protein kinase PBL1	659	689	670	−38.7	−26.2	0.6770026	21	3	0.8580377
cbo-miR37	NODE_178814	cyclin-U1-1	225	244	236	−43.8	−28.7	0.6552511	5.5	4	0.5750046
cbo-miR38	CL400Contig	monodehydroascorbate reductase-like	260	280	271	−22.7	−16.4	0.722467	9.5	4	0.9920018
cbo-miR38	NODE_145275	Ankyrin repeat-containing protein ITN1	220	241	232	−22.7	−15.8	0.6960352	10	4	0.9975505
cbo-miR38	NODE_145474	Calreticulin	181	201	192	−22.7	−18.6	0.8193833	5	2	0.8543774
cbo-miR38	NODE_146660	microfibrillar-associated protein 1-like	64	85	75	−22.7	−16.3	0.7180617	8.5	3	0.9997181
cbo-miR38	NODE_14724	tubulin alpha-3 chain	3	24	15	−22.7	−16.5	0.7268722	10	2	0.987598
cbo-miR38	NODE_163874	ubiquitin-NEDD8-like protein RUB2	206	231	222	−22.7	−17.5	0.7709251	15	4	0.9571649
cbo-miR38	NODE_165185	RNA-dependent RNA polymerase 6	277	297	288	−22.7	−14.9	0.6563877	13	3	0.9999993
cbo-miR38	NODE_166426	probable protein phosphatase 2C 73	128	148	139	−22.7	−15.6	0.6872247	12.5	3	0.9999789
cbo-miR38	NODE_167574	60S ribosomal protein L10a	936	956	947	−22.7	−17.6	0.7753304	11	0	0.5686839
cbo-miR38	NODE_24932	oligoribonuclease isoform X1	745	765	756	−22.7	−14.9	0.6563877	8	4	0.9998352
cbo-miR38	NODE_9848	secretory carrier-associated membrane protein 2-like isoform X1	462	482	473	−22.7	−17.4	0.7665198	7	2	0.9521366
cbo-miR40	NODE_27385	50S ribosomal protein L12, chloroplastic-like	45	71	62	−39	−25.7	0.6589744	21	3	0.7158009
cbo-miR40	NODE_97505	60S ribosomal protein L11-1-like	168	188	179	−39	−25.6	0.6564103	8	3	0.7317734
cbo-miR41	NODE_14995	15.4 kDa class V heat shock protein	281	297	288	−34.6	−22.6	0.6531792	8.5	2	0.5262221
cbo-miR41	NODE_97581	probable GTP diphosphokinase RSH2, chloroplastic	677	693	685	−34.6	−23.1	0.6676301	5.5	3	0.5949696
cbo-miR42	NODE_582	Regulator of rDNA transcription protein 15	169	189	178	−39.5	−25.8	0.6531646	12	3	0.6860944
cbo-miR43	NODE_88402	phosphoenolpyruvate carboxylase	938	957	947	−39.7	−26.1	0.6574307	7.5	3	0.7132207
cbo-miR45	NODE_59631	carbonic anhydrase 2-like isoform X1	139	161	147	−36.3	−24.3	0.6694215	15	3	0.6703943

Table 2
Significant targets identified for the novel miRNAs using from leaf transcriptome by parallel analysis of RNA ends.

Novel miRNA	Transcript ID	Transcript Annotation	T Start	T Stop	T Slice	MFE perfect	MFE site	MFE ratio	Allen Score	DegradomeCategory	DegradomePval
cbo-miR9	800858	heterogeneous nuclear ribonucleoprotein 1	125	141	132	−35	−23.3	0.6657143	5.5	3	0.7180823
cbo-miR10	643000	DUF239 domain-containing protein/DUF4409 domain-containing protein	4	26	17	−48.5	−31.6	0.6515464	7	3	0.5381974
cbo-miR11	777754	uncharacterised protein LOC105046047	132	146	139	−31.3	−20.5	0.6549521	6	4	0.7860629
cbo-miR11	808092	glycerate dehydrogenase	370	387	378	−31.3	−21.3	0.6805112	6	2	0.5109217
cbo-miR12	762472	ribonuclease P protein subunit p25-like	134	153	143	−40.1	−26.5	0.6608479	9.5	3	0.9359704
cbo-miR12	809118	protein SUPPRESSOR OF QUENCHING 1, chloroplastic	128	148	137	−40.1	−29.1	0.7256858	8	3	0.5808894
cbo-miR14	726426	cysteine proteinase inhibitor 1	70	90	81	−37.4	−24.4	0.6524064	10.5	2	0.5939686
cbo-miR16	796780	predicted protein	234	252	243	−34.6	−22.7	0.6560694	8	4	0.5229991
cbo-miR16	812990	phenylalanine *N*-monooxygenase	637	655	646	−34.6	−22.5	0.650289	8.5	3	0.7437088
cbo-miR17	752156	magnesium protoporphyrin IX methyltransferase, chloroplastic	43	70	55	−44.3	−28.8	0.6501129	18.5	2	0.7879149
cbo-miR18	767182	putative transferase At4g12130, mitochondrial	102	123	112	−36	−24.1	0.6694444	7	4	0.6795481
cbo-miR19	621385	unknown protein	62	81	72	−34	−23.8	0.7	7.5	3	0.7681924
cbo-miR20	790936	protein TPR2-like	110	129	119	−35.2	−23.2	0.6590909	9	3	0.8698097
cbo-miR20	809674	UDP-xylose transporter 3	374	393	383	−35.2	−23.2	0.6590909	7	4	0.7005736
cbo-miR21	795302	calcium sensing receptor, chloroplastic	309	331	317	−35.4	−24	0.6779661	12.5	3	0.7852817
cbo-miR21	815674	protein OBERON 3	507	525	515	−35.4	−24.1	0.680791	7.5	4	0.5959603
cbo-miR22	813994	homogentisate 1,2-dioxygenase	28	50	39	−34.9	−22.9	0.6561605	8.5	3	0.9382182
cbo-miR23	784094	alanine–glyoxylate aminotransferase 2 homolog 1, mitochondrial	153	172	163	−32.6	−21.6	0.6625767	7.5	4	0.5000536
cbo-miR24	715030	probable mannitol dehydrogenase	1	21	11	−33.8	−22.1	0.6538462	9	0	0.6135232
cbo-miR24	753730	50S ribosomal protein L29, chloroplastic	52	71	62	−33.8	−22.5	0.6656805	6.5	4	0.9233405
cbo-miR24	805134	ABC transporter F family member 5	189	211	201	−33.8	−24.5	0.7248521	8.5	4	0.6059587
cbo-miR25	799828	photosystem I reaction center subunit III, chloroplastic	381	399	390	−30.2	−19.9	0.6589404	10.5	3	0.5559239
cbo-miR26	763586	protein MAIN-LIKE 1-like	42	62	53	−29	−19	0.6551724	9.5	2	0.7663572
cbo-miR26	786474	photosystem I reaction center subunit N, chloroplastic	166	184	175	−29	−20.4	0.7034483	10.5	3	0.5976624
cbo-miR26	809712	START domain-containing protein	110	128	119	−29	−20.1	0.6931034	9.5	3	0.6940868
cbo-miR26	813610	phenylalanine–tRNA ligase, chloroplastic/mitochondrial	166	184	175	−29	−19.4	0.6689655	7	4	0.6996343
cbo-miR27	788578	ATP synthase subunit alpha, mitochondrial-like	220	237	229	−30.6	−20	0.6535948	10	4	0.7708012
cbo-miR27	800314	NAD(P)H-quinone oxidoreductase subunit U, chloroplastic	73	93	84	−30.6	−21.3	0.6960784	7.5	3	0.6464748
cbo-miR28	745646	50S ribosomal protein L29, chloroplastic-like	24	42	32	−26	−17.3	0.6653846	7	2	0.6887955
cbo-miR28	794310	ornithine carbamoyltransferase, chloroplastic	4	21	12	−26	−17.4	0.6692308	6	3	0.8717885
cbo-miR28	801938	endoglucanase 10-like	224	243	233	−26	−17.4	0.6692308	7	2	0.6660672
cbo-miR28	804044	50S ribosomal protein L19-2, chloroplastic	204	222	212	−26	−18	0.6923077	9	3	0.7103006
cbo-miR30	808092	glycerate dehydrogenase	368	385	376	−29	−20.2	0.6965517	6.5	3	0.5886621
cbo-miR30	809620	dynein light chain LC6, flagellar outer arm	112	131	120	−29	−19.5	0.6724138	9.5	3	0.8167119
cbo-miR32	806672	histone deacetylase HDT2-like	34	56	47	−32.3	−21.8	0.6749226	12	3	0.8916678
cbo-miR32	814714	glutamine synthetase leaf isozyme, chloroplastic	585	602	594	−32.3	−21.1	0.6532508	8	4	0.8818904
cbo-miR33	776252	ferredoxin–NADP reductase, leaf isozyme, chloroplastic	83	101	92	−22.5	−14.7	0.6533333	10	4	0.7067612
cbo-miR33	813060	ribosome-recycling factor, chloroplastic	85	102	93	−22.5	−15.2	0.6755556	7	2	0.5200292
cbo-miR34	627576	ras-related protein Rab 7	8	25	16	−31.6	−21.3	0.6740506	7.5	3	0.5914527
cbo-miR34	740062	Tubulin beta-2 chain	41	57	49	−31.6	−20.9	0.6613924	5	3	0.6977094
cbo-miR34	793294	Histone-lysine *N*-methyltransferase ATX2	174	190	181	−31.6	−20.6	0.6518987	7.5	4	0.6136983
cbo-miR34	809328	putative LOV domain-containing protein	257	276	267	−31.6	−21.5	0.6803797	9	3	0.5581853
cbo-miR35	666605	protein NLP2	65	81	73	−34.4	−22.5	0.6540698	9.5	3	0.5413303
cbo-miR36	807370	probable serine/threonine-protein kinase PBL1	416	446	427	−38.7	−26.2	0.6770026	21	3	0.7613881
cbo-miR38	670589	Proton-dependent oligopeptide transporter family	4	24	15	−22.7	−15	0.660793	11	3	0.9999858
cbo-miR38	759654	clathrin light chain 1-like	94	116	107	−22.7	−17.3	0.7621145	9	3	0.9898101
cbo-miR38	764292	DEAD-box ATP-dependent RNA helicase 42	52	72	63	−22.7	−20.2	0.8898678	5.5	3	0.7552186
cbo-miR38	770506	Cytochrome P450 90B1	3	24	14	−22.7	−15.8	0.6960352	8	3	0.9996997
cbo-miR38	786474	photosystem I reaction center subunit N, chloroplastic	56	76	67	−22.7	−16.6	0.7312775	11	3	0.9974672
cbo-miR38	786590	transketolase, chloroplastic	41	61	52	−22.7	−15.8	0.6960352	12	2	0.9898499
cbo-miR38	790618	AT hook-containing MAR binding 1-like protein	76	100	91	−22.7	−18.3	0.8061674	12	4	0.8480987
cbo-miR38	791696	probable protein phosphatase 2C 73	123	143	134	−22.7	−15.6	0.6872247	12.5	3	0.9998726
cbo-miR38	794840	sphingosine kinase 1-like	139	159	150	−22.7	−15.2	0.6696035	10	0	0.8632381
cbo-miR38	796256	secretory carrier-associated membrane protein 2-like isoform X1	294	314	305	−22.7	−17.4	0.7665198	7	2	0.9129919

(*continued on next page*)

Table 2 (*continued*)

Novel miRNA	Transcript ID	Transcript Annotation	T Start	T Stop	T Slice	MFE perfect	MFE site	MFE ratio	Allen Score	DegradomeCategory	DegradomePval
cbo-miR38	802366	oligoribonuclease isoform X1	186	206	197	−22.7	−14.9	0.6563877	8	4	0.9992124
cbo-miR38	804382	(+)-neomenthol dehydrogenase-like isoform X2	290	313	301	−22.7	−16.3	0.7180617	12.5	2	0.9779391
cbo-miR38	811922	furostanol glycoside 26-O-beta-glucosidase-like	50	70	61	−22.7	−16.1	0.7092511	8.5	3	0.9992992
cbo-miR38	812020	structural maintenance of chromosomes protein 1	649	675	660	−22.7	−18	0.7929515	15	3	0.9701275
cbo-miR39	816040	heat shock 70 kDa protein 17	221	244	231	−33.9	−22.3	0.6578171	14	3	0.5872597
cbo-miR44	792896	protein ECERIFERUM 26-like	126	143	134	−35.3	−23.2	0.6572238	8.5	4	0.5698403
cbo-miR45	769236	protein FAR1-RELATED SEQUENCE 6 isoform X1	25	42	33	−36.3	−25.1	0.6914601	6.5	3	0.5056669

transcriptome. Similarly 29 novel miRNAs were targeting 50 transcripts from root transcriptome (Fig. 1). Some miRNAs had targets in both root and leaf. This shown that multiple miRNAs had more than one target and vice versa. Then degradome categories explored for cleavage sites and 3, 0, 22, 77 and 44 number of targets fell under 0, 1, 2, 3, 4 categories respectively. cbo-miR24 and cbo-miR38 are targeting mRNAs transcripts coding for manitol dehydrogenase, sphingosine kinase 1-like, 60S ribosomal protein.

More exact complementarity between miRNA and corresponding mRNA in plants make target identification more precise. Furthermost, plant miRNAs mainly show complementarity in coding region. It is key merit useful for degradome approach and to distinguish novel miRNAs on the basis of their roles [21]. Total 45,702,108 reads were obtained from degradome sequencing and after trimming we got 14,726,700 reads of > 16bp length. Previously reported all novel miRNAs along with novel miRNAs identified in current study and the leaf and root transcriptome data of *C. borivilianum* was used as input for the degradome analysis. Targets having significant p-value (≥ 0.5) were used for further exploration. Table 1 and Table 2 consists of description of all novel miRNAs targeting root and leaf transcripts respectively of *C. borivilianum*.

Novel miRNA cbo-miR38 was found to have the maximum in both root and leaf in *C. borivilianum* leaf (14 targets) and root (11 targets). Leaf targets were annotated as Proton-dependent oligopeptide transporter family, clathrin light chain 1-like, DEAD-box ATP-dependent RNA helicase 42, Cytochrome P450 90B1, photosystem I reaction center subunit N, chloroplastic, transketolase, chloroplastic, AT hook-containing MAR binding 1-like protein, probable protein phosphatase 2C 73, sphingosine kinase 1-like, secretory carrier-associated membrane protein 2-like isoform X1, oligoribonuclease isoform X1, (+)-neomenthol dehydrogenase-like isoform X2, furostanol glycoside 26-O-beta-glucosidase-like.

Structural maintenance of chromosomes protein 1. Whereas the root transcript targets were annotated as monodehydroascorbate reductase-like, Ankyrin repeat-containing protein ITN1, Calreticulin, microfibrillar-associated protein 1-like, tubulin alpha-3 chain, ubiquitin-NEDD8-like protein RUB2, RNA-dependent RNA polymerase 6, probable protein phosphatase 2C 73, 60S ribosomal protein L10a, oligoribonuclease isoform X1, secretory carrier-associated membrane protein 2-like isoform X1. This showed the role of cbo-miR38 in secondary metabolism, miRNA biogenesis and photosynthetic light reaction etc. Surprisingly, we found cbo-miR38 targeting photosystem I. To best of our knowledge, till now no miRNA is reported targeting Photosystem I reaction center subunit. The pigments present in Photosystem I and photosystem II produce photons by using light energy that ultimately form energy compounds in plants [22]. From this study we also endorse the earlier well-known assumption that state multiple role of a single miRNA conclude alteration in one metabolic process due to the consequences of other. Like effect of photosynthesis on the grain size in plants [23].

2.2.1. Gene ontology study of targets

Functional annotation of target genes was carried out by using Blast2GO 5. Selectively total 109 (50 from root and 59 from leaf) targets predicted by degradome sequencing were subjected to BLAST2GO. Selected target sequences were mapped with GO database. These transcripts were classified into three major categories namely biological process, molecular function and cellular components using plant specific GO slims. Functional classification of *C. borivilianum* targets from root tissue in biological process category showed maximum targets involved in metabolic process (GO:0008152), cellular process (GO:0009987), and cellular component organization and biogenesis (GO:0071840). Some of the targets were also found to participate in biological regulation, localization, regulation of biological processes [Fig. 2(A)]. This suggested the gross entailing of identified targets in plant growth and metabolic activity. In cellular component group target

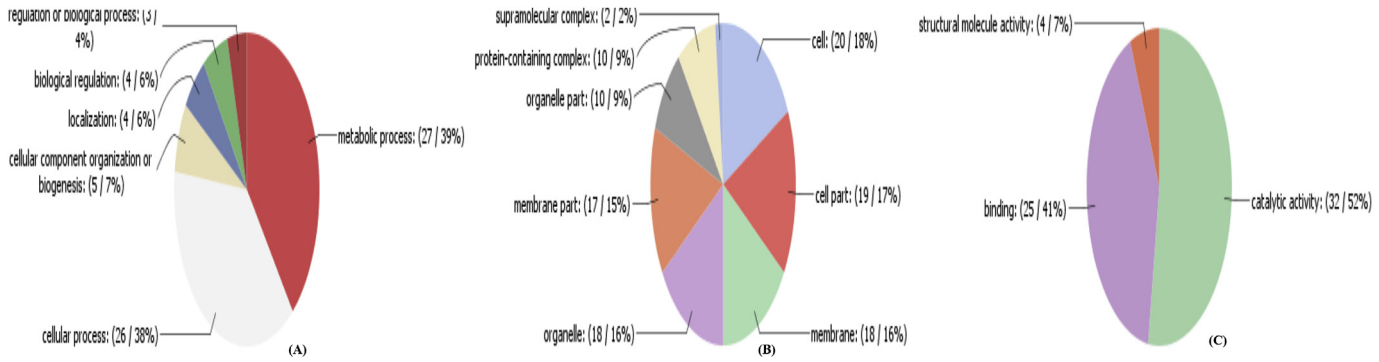

Fig. 2. Categorization of root target genes according to (A) Biological processes (B) Cellular components (C) molecular function.

sequences related to cell (GO:0005623), cell part (GO:0044464), membrane (GO:0016020) and organelle (GO:0043226) were maximum [Fig. 2(B)]. The targets belonging to major subgroup of molecular function category included binding (GO:0005488), catalytic activity (GO:0003824) and structural molecular activity (GO:0005158) [Fig. 2(C)].

Functional classification of *C. borivilianum* targets from root tissue in biological process category showed maximum targets involved in cellular process (GO:0009987), metabolic process (GO:0008152) and biological regulation (GO:0065007). Some of the targets were also found to contribute in regulation of biological processes, cellular component regulation and biogenesis, response to stimulus, localization, development process, and multicellular organismal process [Fig. 3(A)]. In cellular component group target sequences related to cell (GO:0005623), cell part (GO:0044464), and organelle (GO:0043226) were maximum [Fig. 3(B)]. The targets belonging to major subgroup of molecular function category included binding (GO:0005488), catalytic activity (GO:0003824) and structural molecular activity (GO:0005158) [Fig. 3(C)].

Further to analyze the role of identified target transcripts, they were mapped to KEGG pathway. Total 50 targets in *C. borivilianum* root transcriptome were involved in 36 metabolic networks including Fatty acid degradation, Biosynthesis of unsaturated fatty acids, alpha-Linolenic acid metabolism, Nitrogen metabolism, Biosynthesis of antibiotics, Glyoxylate and dicarboxylate metabolism, Methane metabolism, Pyruvate metabolism, Carbon fixation pathways in prokaryotes, Carbon fixation in photosynthetic organisms, Various types of *N*-glycan biosynthesis, *N*-Glycan biosynthesis, Alanine, aspartate and glutamate metabolism, Cysteine and methionine metabolism, Glycine, serine and threonine metabolism, Starch and sucrose metabolism, Biosynthesis of antibiotics, Citrate cycle (TCA cycle), Glycolysis/Gluconeogenesis, Pyruvate metabolism, Purine metabolism, Amino sugar and nucleotide sugar metabolism, Thiamine metabolism, Purine metabolism, Oxidative phosphorylation, Photosynthesis, Biosynthesis of ansamycins, Biosynthesis of antibiotics, Pentose phosphate pathway, Carbon fixation in photosynthetic organisms, Valine, leucine and isoleucine degradation, Ascorbate and aldarate metabolism, Amino sugar and nucleotide sugar metabolism, Other glycan degradation, Galactose metabolism, Glycosaminoglycan degradation, Glycosphingolipid biosynthesis - ganglio series, Sphingolipid metabolism, Oxidative phosphorylation, T cell receptor signaling pathway, PD-L1 expression and PD-1 checkpoint pathway in cancer, Th1 and Th2 cell differentiation, Glycerophospholipid metabolism. Similarly, 59 targets in *C. borivilianum* leaf transcriptome were involved in 23 metabolic networks including Monoterpenoid biosynthesis, Alanine, aspartate and glutamate metabolism, Cysteine and methionine metabolism, Glycine, serine and threonine metabolism, Starch and sucrose metabolism, Purine metabolism, Tyrosine metabolism, Styrene degradation, Purine metabolism, Thiamine metabolism, Porphyrin and chlorophyll metabolism, Biosynthesis of antibiotics, Arginine biosynthesis, Photosynthesis, Biosynthesis of antibiotics, Biosynthesis of ansamycins, Pentose phosphate pathway, Carbon fixation in photosynthetic organisms, Valine, leucine and isoleucine degradation, Aminoacyl-tRNA biosynthesis, Glyoxylate and dicarboxylate metabolism, Nitrogen metabolism, Arginine biosynthesis, Alanine, aspartate and glutamate metabolism. The details of all identified metabolic pathways mentioned in from root and leaf are mentioned in Table 3 and Table 4 respectively. Activation of photosynthesis in leaf is regulated by cbo-miR33 whereas in root inactivation of the same involve 2 miRNAs i.e. cbo-miR24 and cbo-miR33. These 2 plant specific miRNAs target transcript coding for FNR (PetH) reductase (ec:1.18.1.2 – reductase) involved in photosynthesis electron transport in Photosystem II (Fig. 4). Oxidative phosphorylation in root is regulated by 2 miRNAs. ec:7.1.1.2 - reductase (H + -translocating) and ec:1.6.99.3 – dehydrogenase are targeted by cbo-miR19. Whereas ec:3.6.1.1 – diphosphatase is targeted by cbo-miR9 (Fig. 5). This analysis showed the wide involvement of miRNAs in all above mentioned biological processes (see Table 5).

On the basis of above analysis, we confirmed the existence of 40

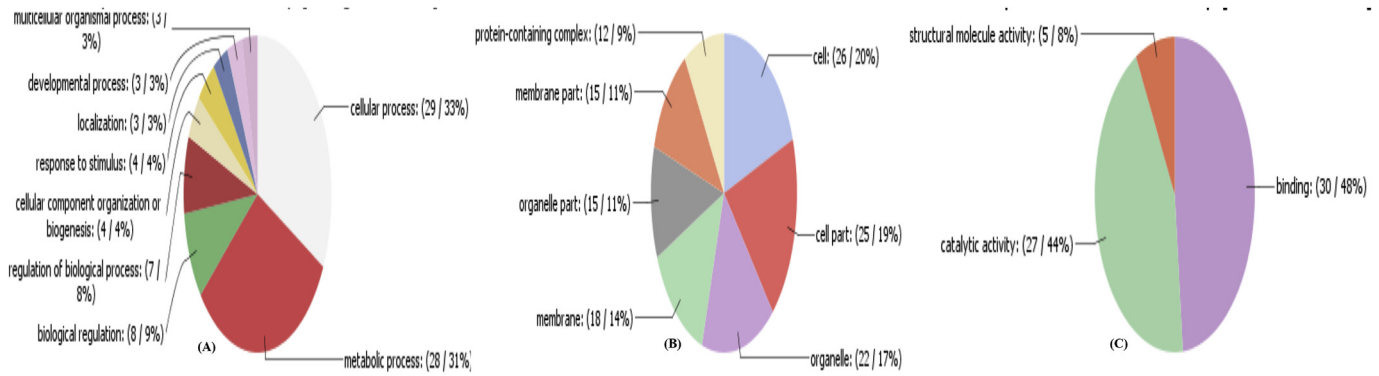

Fig. 3. Categorization of leaf target genes according to (A) Biological processes (B) Cellular components (C) molecular function.

Table 3
Description of novel miRNA profile from *C. borivilianum*.

miRNA ID	Novel miRNA sequence	Length	Frequency	STRAND	MFE VALUE (Kcal/mol)	G-C Percent
cbo-miR6	AGAAGCTTTGATACCATTT	19	1	+	−32.40	31.51%
cbo-miR7	AGAGATGGGTGAGAAGAG	18	2	–	−45.30	60.71%
cbo-miR8	AGAGATGGGTGAGAAGAGGG	20	26	–	−45.30	60.71%
cbo-miR9	AGATGGGTGAGAAGAGGG	18	2	–	−45.30	0.6071
cbo-miR10	ACGGGCGCTGGCTGCAGGGC	20	2	–	−65.00	0.7895
cbo-miR11	GGGTCTGTTTGGTTTGAG	18	1	+	−30.20	0.4545
cbo-miR12	TCTGCTGTGCTGCTGCTGC	19	3	–	−35.30	0.6508
cbo-miR13	TCTCGGGCCAGGCTTCATT	19	2	+	−43.60	50.51%
cbo-miR14	ATCGTGCCGTGCCGTGCT	18	1	–	−56.40	0.5556
cbo-miR15	TCGTGTCGTGCCGTGCTGGC	20	1	+	−60.30	79.07%
cbo-miR16	TGTGTTCTCAGGTCGCCT	18	1	–	−65.40	0.6264
cbo-miR17	CTCTCTCTCTCTCTCGGCCTC	21	1	–	−65.40	0.6264
cbo-miR18	GAAGGGATTTGGAGGGGAT	19	1	+	−36.40	0.4615
cbo-miR19	AAGGGATTTGGAGGGGATT	19	1	+	−36.40	0.4615
cbo-miR20	GACGGATTTGGAGGGGATT	19	1	–	−37.50	0.359
cbo-miR21	AGGGATTTGGAGGGGACT	18	1	–	−37.50	0.359
cbo-miR22	AGGGATTTGGAGGGGATTTT	20	1	+	−50.80	0.4773
cbo-miR23	AGGAGATGGTTCATGCTG	18	2	+	−32.10	0.3182
cbo-miR24	TCTCTTCTTCATCTCTCTCT	20	5	+	−30.60	0.3678
cbo-miR25	ATATGTTGGGTTTGACGTG	19	1	–	−38.10	0.4565
cbo-miR26	AAAGGTTGAGCTCTTTTCA	19	3	+	−38.90	0.3407
cbo-miR27	GTTTCGTTTCGGTTTCGGT	19	1	+	−43.50	0.382
cbo-miR28	GTTTGGTTCGGATTTTTC	18	1	–	−35.10	0.4416
cbo-miR29	ATTCGGTTCGGTTTGGAT	18	1	–	−41.40	48.89%
cbo-miR30	TTCGGTTCGGTTTGGATT	18	1	–	−41.40	0.4889
cbo-miR31	TCTCTTCTTCATCTCTCTCT	20	5	–	−32.70	37.14%
cbo-miR32	AAGGAAGGAGAGAGAGATT	19	1	–	−32.70	0.3714
cbo-miR33	TAGACTGTCTTTATTTTTT	19	4	+	−31.20	0.3684
cbo-miR34	GCACGATCTGGAGCTTTT	18	1	–	−44.70	0.4588
cbo-miR35	TTCGACTGAAGGGAGCTC	18	1	–	−32.20	0.3864
cbo-miR36	GAGAGAGAGAGAGAGAAGGTT	21	1	–	−32.30	0.3194
cbo-miR37	GAGAGAGAGAGAGAAGGGTCGA	22	2	–	−32.30	31.94%
cbo-miR38	CTTTCTTTCTTTCTTTTTTTT	21	1	–	−32.30	0.3194
cbo-miR39	TTGGCATTCTGTCCACCTT	19	1	–	−42.30	0.4624
cbo-miR40	TTGGCTTTCTGTCCACCTCC	20	1	–	−42.30	46.24%
cbo-miR41	TGTGTTCTCAGGTCGCCT	18	1	+	−49.60	56.67%
cbo-miR42	GGCATGTTGGCTGGCTCGA	19	2	+	−48.50	46.46%
cbo-miR43	GGGATGTTGGCTGGCTCGA	19	2	+	−48.50	46.46%
cbo-miR44	GATGTCGCCGAGGATGTG	18	23	+	−48.10	0.5934
cbo-miR45	TGTCGCCGAGGATGTGCT	18	3	+	−48.10	0.5934

novel miRNAs out of total 2144 predicted. These novel miRNAs were confirmed on the basis of their targets in from leaf and root transcriptome by degradome sequencing analysis. These 40 novel miRNAs were named from cbo-miR6 to cbo-miR45 on the basis of well-known nomenclature criteria [24]. cbo-miR6 was found to have transcript matching to *A. thaliana*. cbo-miR7 to cbo-miR23 were having their precursor from *O. sativa*, cbo-miR29 and cbo-miR30 from *P. trichocarpa*, cbo-miR31 to cbo-miR38 from *R. communis*, and cbo-miR39 to cbo-miR45 from *V. vinifera* (Table 3). Secondary structures were predicted for the precursor sequence of the all confirmed miRNAs (supplementary File 6). This was to our surprise that only one novel miRNAs was corresponding to *A. thaliana* was having any potential target in *C. borivilianum*. This suggested that even if both *C. borivilianum* and *A. thaliana* belongs to monocot, they have the very less similarity at miRNAs level. Gene regulation have involve majorly different mechanism in both plants in comparison to others.

The low abundance of novel miRNAs was in the range from 1 to 26. The abundance of cbo-miR8 was maximum followed by cbo-miR44. Apart from this multiple miRNAs with only 1 read count were also identified (Fig. 6(a)). The range of the length of novel miRNAs was from 18 to 22 (Fig. 6(b)). Abundance of novel miRNAs of length 18 nt was maximum. Novel miRNAs of length 24 nt used be most abundant among plant species. The same was not observed in the present case. This might be due to unavailability of plant's own genome. Once the genome sequence will be available, variability of 3′ end of miRNA can be assured in future. Further, no significant result after BLASTN of novel miRNAs confirmed their novelty. These *C. borivilianum* specific miRNAs were having their origin from both plus and minus strand of precursor, but more from minus strand.

3. Discussion

Since the time of Ayurvedic medicine, mainly 13 Indian species of Chlorophytum have been reported such as C. arundinaceum Baker, C. attenuatum Baker, C. breviscapum Dalz, C. borivilianum Sant and Fern, C. glaucum Dalz, C. orcbidastrum Lindley, C. kbasianum Hooker, C. undulatum Wall, C. Laxum R. Br., C. tuberosum Baker, and C. malabaricum Baker [25–27]. C. borivilianum is best known for cultivation purpose as it gives good returns with less inputs. Per hectare production of C. borivilianum varies from 40 to 50 quintal per hectare. The presence of pathways like Saponin Biosynthesis, Flavonoid Biosynthesis, and Alkaloid Biosynthesis, responsible to incorporate uniqueness in medicinal plants. Secondary metabolites like saponins act as antioxidant and helps in reduction of free radicals. Saponins possess properties like sweetness to bitterness, foaming, emulsification, pharmacological, medicinal, haemolytic, antimicrobial, insecticidal, molluscicidal activities, and find some place in cosmetic industry, beverages, and confectionery [28]. Saponins are present in high amounts in a variety of plant species like C. borivilianum, Glycyrrhiza glabra, Panax ginseng, Bacopa monnieri, and Ilex paraguariensis [29]. Steroidal saponins are mainly known as the principal bioactive components responsible for the therapeutic properties of C. borivilianum. The initial steps for their biosynthesis in plants involve both mevalonic acid (MVA) pathway and 2-*C*-methyl-Derythritol-4-phosphate (MEP) pathway,

Table 4
Details of all identified KEGG pathways involved root targets.

Enzyme	Pathway	Pathway ID	#Enzs in Pathway	#Seqs in Pathway	Trascript ID
ec:1.3.3.6 - oxidase	Fatty acid degradation, Biosynthesis of unsaturated fatty acids, alpha-Linolenic acid metabolism	map 00071, map 01040, map 00592	1, 1, 1	1	NODE_153391
ec:4.2.1.1 - anhydrase	Nitrogen metabolism	map00910	1	1	NODE_59631
ec:1.1.3.15 - oxidase	Biosynthesis of antibiotics, Glyoxylate and dicarboxylate metabolism	map01130, map00630	3, 1	1	NODE_127333
ec:4.1.1.31 - carboxylase	Methane metabolism, Pyruvate metabolism, Carbon fixation pathways in prokaryotes, Carbon fixation in photosynthetic organisms	map 00680, map00620, map 00720, map00710	1, 2, 1, 2	1	NODE_88402
ec:2.4.1.132 - alpha-1,3-mannosyltransferase	Various types of *N*-glycan biosynthesis, *N*-Glycan biosynthesis	map 00513, map 00510	1, 1	1	NODE_159321
ec:2.6.1.44 - transaminase	Alanine, aspartate and glutamate metabolism, Cysteine and methionine metabolism, Glycine, serine and threonine metabolism	map00250, map00270, map00260	1, 1, 1	1	NODE_52274
ec:3.2.1.1 - glycogenase	Starch and sucrose metabolism	map00500	1	1	NODE_5941
ec:4.1.1.32 - carboxykinase (GTP)	Biosynthesis of antibiotics, Citrate cycle (TCA cycle), Glycolysis/Gluconeogenesis, Pyruvate metabolism	map01130, map 00020, map 00010, map00620	3, 1, 1, 2	1	NODE_88402
ec:3.6.1.3 - adenylpyrophosphatase	Purine metabolism	map00230	2	2	NODE_161012, NODE_146239
ec:2.4.1.43 - 4-alpha-galacturonosyltransferase	Amino sugar and nucleotide sugar metabolism	map00520	2	1	NODE_169749
ec:3.6.1.15 - phosphatase	Thiamine metabolism, Purine metabolism	map00730, map00230	1, 2	3	NODE_161012
ec:7.1.1.2 - reductase (H + -translocating)	Oxidative phosphorylation	map00190	3	1	NODE_160962
ec:1.18.1.2 - reductase	Photosynthesis	map00195	1	2	NODE_57190
ec:2.2.1.1 - glycolaldehydetransferase	Biosynthesis of ansamycins, Biosynthesis of antibiotics, Pentose phosphate pathway, Carbon fixation in photosynthetic organisms	map01051, map01130, map00030, map00710	1, 3, 1, 2	1	NODE_135485
ec:2.6.1.40 - transaminase	Valine, leucine and isoleucine degradation	map00280	1	1	NODE_52274
ec:5.1.3.18–3,5-epimerase	Ascorbate and aldarate metabolism, Amino sugar and nucleotide sugar metabolism	map 00053, map00520	1, 2	1	NODE_12903
ec:3.2.1.23 - lactase (ambiguous)	Other glycan degradation, Galactose metabolism, Glycosaminoglycan degradation, Glycosphingolipid biosynthesis - ganglio series, Sphingolipid metabolism	map 00511, map 00052, map 00531, map 00604, map 00600	1, 1, 1, 1, 1	1	NODE_159279
ec:1.6.99.3 - dehydrogenase	Oxidative phosphorylation	map00190	3	1	NODE_160962
ec:3.1.3.16 - phosphatase	T cell receptor signaling pathway, PD-L1 expression and PD-1 checkpoint pathway in cancer, Th1 and Th2 cell differentiation	map04660, map05235, map04658	1, 1, 1	1	NODE_166426
ec:3.6.1.1 - diphosphatase	Oxidative phosphorylation	map00190	3	1	NODE_3011
ec:2.1.1.103 - *N*-methyltransferase	Glycerophospholipid metabolism	map 00564	1	1	NODE_171312

Table 5
Details of all identified KEGG pathways involved leaf targets.

Enzyme	Pathway	Pathway ID	#Enzs in Pathway	#Seqs in Pathway	Transcript ID
ec:1.1.1.208 - dehydrogenase	Monoterpenoid biosynthesis	map 00902	1	1	804382
ec:2.6.1.44 - transaminase	Alanine, aspartate and glutamate metabolism, Cysteine and methionine metabolism, Glycine, serine and threonine metabolism	map00250, map00270, map00260	2, 1, 1	1	784094
ec:3.2.1.4 - endo-1,4-beta-D-glucanase	Starch and sucrose metabolism	map00500	1	1	801938
ec:3.6.1.3 - adenylpyrophosphatase	Purine metabolism	map00230	2	2	805134, 809620
ec:1.13.11.5–1,2-dioxygenase	Tyrosine metabolism, Styrene degradation	map 00350, map 00643	1, 1	1	813994
ec:3.6.1.15 - phosphatase	Purine metabolism, Thiamine metabolism	map00230, map00730	2, 1	3	805134, 809620, 627576
ec:2.1.1.11 - protoporphyrin IX methyltransferase	Porphyrin and chlorophyll metabolism	map 00860	1	1	752156
ec:2.1.3.3 - carbamoyltransferase	Biosynthesis of antibiotics, Arginine biosynthesis	map01130, map00220	2, 2	1	794310
ec:1.18.1.2 - reductase	Photosynthesis	map00195	1	1	776252
ec:2.2.1.1 - glycolaldehydetransferase	Biosynthesis of antibiotics, Biosynthesis of ansamycins, Pentose phosphate pathway, Carbon fixation in photosynthetic organisms	map01130, map01051, map00030, map00710	2, 1, 1, 1	1	786590
ec:2.6.1.40 - transaminase	Valine, leucine and isoleucine degradation	map00280	1	1	784094
ec:6.1.1.20 - ligase	Aminoacyl-tRNA biosynthesis	map 00970	1	1	813610
ec:3.1.3.16 - phosphatase	Th1 and Th2 cell differentiation, T cell receptor signaling pathway, PD-L1 expression and PD-1 checkpoint pathway in cancer	map04658, map04660, map05235	1, 1, 1	1	791696
ec:6.3.1.2 - synthetase	Glyoxylate and dicarboxylate metabolism, Nitrogen metabolism, Arginine biosynthesis, Alanine, aspartate and glutamate metabolism	map00630, map00910, map00220, map00250	1, 1, 2, 2	1	814714

located in cytosol and plastids, respectively. These pathways in C. borivilianum were well illustrated by various transcriptome studies [6]. Genes involved in initial steps of saponin biosynthesis are more active in leaf tissue whereas later step genes show more expression in root tissue of the plant [7–9]. Different formulations of root extract of C. borivilianum shown diverse actions like crude extract have higher antioxidant activity and bleaching activity while saponin filtrate shown greater ferrous ion chelating activity. MTT cell viability assay using MCF-7, PC3, and HCT-116 cancer cell lines proved that crude extract has more cytotoxic activity than total saponin extract. C. borivilianum polysaccharide intake at 0.4% for 4 weeks enhance resistance ability in Labeo rohita against bacteria Aeromonas hydrophila. This was evident by increasing level of 4 pro-inflammatory cytokines (IL-8, IL-1β, iNOS, and TNF-α) and decrease in 2 anti-inflammatory cytokines (IL-10 and TGF-β) level [30]. It was also reported by a study on the pancreatic tissue of diabetic rats that C. borivilianum root extract affects lipid panel, insulin amount, blood sugar regulation, and reduce oxidative stress [31]. The root extract of C. borivilianum have physiochemical potential to reduce the rate of corrosion of steel when applied in the acidic medium [32]. These all studies portray a sound picture how beneficial C. borivilianum is for human kind. Due to immense therapeutic worth of this herb, it was adopted as crop plant from wild long ago. Various methods for its propagation were also developed. Still it have a high market demand and boost in its yield is the requisite of time. Till now efforts were made to increase yield by various modification in propagation methods. But the molecular study opened the way forward for the same at molecular level.

The advancement of molecular studies verified the contribution of miRNAs in controlling the plant metabolism with high specificity at the both transcriptional and post-transcriptional level. These can be used as a potential molecules to improve plant productivity [16]. The gene silencing by mRNA cleavage is most widely observed mode of action of miRNAs [13]. Interference in the translation without altering the level of mRNA is another way [33]. miRNA can target translation at various stages like ribosome stalling, and ribosome unloads but it is more common in animals [34]. Methylation of cytosine at DNA level and obstruction in transcription includes chromatin-modifying enzymes selected by AGO protein, RNA polymerase V and miRNA. This is also known as RNA-directed DNA methylation (RdDM) [35,36]. The present study will act as a supplement to our previous study and help in enhancing understanding related to the miRNA regulation in *C. borivilianum* herb.

3.1. miRNAs and their relative targets

A large pool of 38,589 miRNAs is available from various plants in miRBase 22.1 [37]. A number of them are uncharacterised. Without knowing functional aspect of miRNAs, it is of least importance. This triggered us to study the entire miRNAs pool of *C. borivilianum* along with their targets. From degradome profiling, a wide range of targets found for miRNAs in *C. borivilianum*. In this study we tried to touch every general aspect that a plant specific miRNA can regulate. Single miRNA can participate in multiple regulatory pathways, for instance organ development, vegetative-reproductive phase transition, stress response etc. [38]. Any alteration in the miRNA biogenesis can cause changes in multiple phenotypic traits. From a number of studies, it is well known that miRNA* also act along with miRNA and regulate intracellular activity [39,40].

Root is an essential plant organ that helps in nutrient and H_2O uptake, also provide mechanical strength, and store secondary metabolites [41]. cbo-miR45 target the transcript coding for carbonic anhydrase 2-like isoform X1 in root tissue. Carbonic anhydrase, popularly existing enzyme that catalyse the reversible hydration reaction of CO_2 into bicarbonate. KEGG pathway analysis suggested role of plant specific cbo-miR45 in nitrogen metabolism in *C. borivilianum* root. Role of miRNAs in nitrogen metabolism is well established in plants. Previously

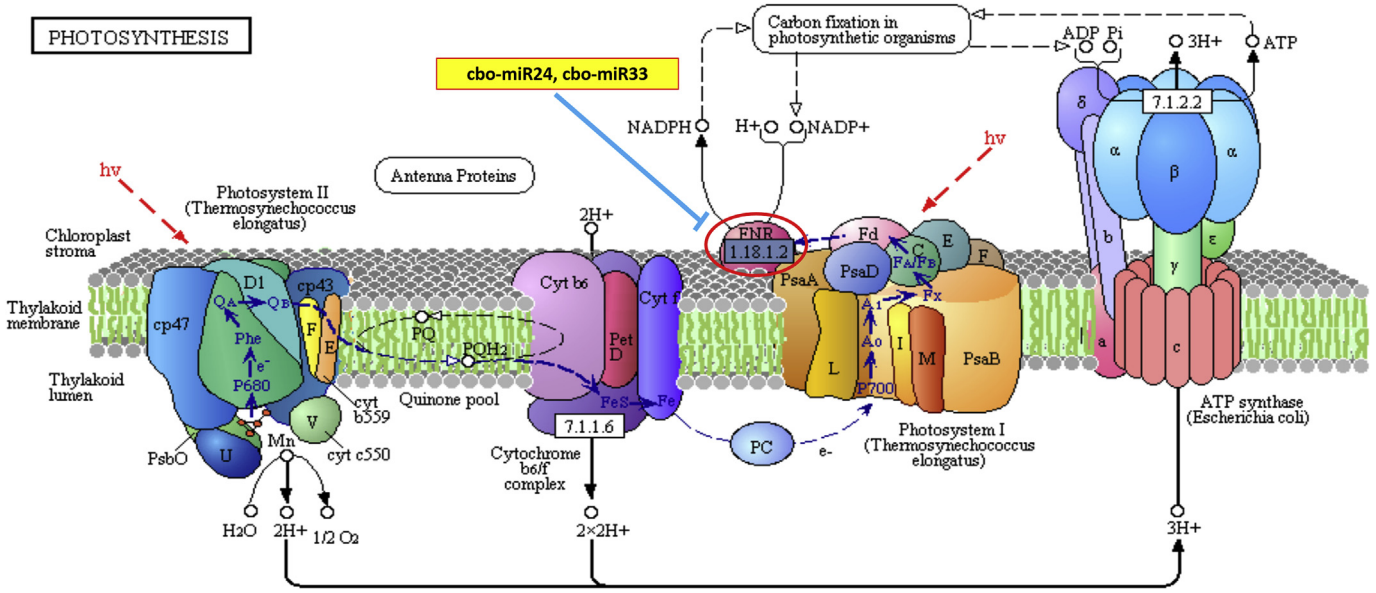

Fig. 4. Pictorial representation of novel miRNAs targeting photosynthesis in both leaf and root tissue of *C. borivilianum* (ec:1.18.1.2 – reductase).

miR171 and miR 397 were found to be involved in nodulation for nitrogen fixation in the Legume *Lotus japonicas* [42]. Apart from miRNA, siRNAs are also reported to target carbonic anhydrase [43]. cbo-miR32 target leaf transcript coding for glutamine synthetase leaf isozyme, chloroplastic in *C. borivilianum*. This is involved in Glyoxylate and dicarboxylate metabolism, Nitrogen metabolism, biosynthesis of Arginine, Aspartate, Alanine, and Glutamate metabolism. In a report, miR 156, miR 159, and miR171 families were found to target mRNA coding for enzymes participating in amino acid, fatty acid, and lipid metabolism in *Arachis hypogaea* L. (peanut) [44]. Present study shown involvement of novel miRNAs in a few developmental processes as their target genes encode for the probable protein phosphatase 2C, secretory carrier-associated membrane protein 2-like isoform X1, oligoribonuclease isoform X1, (+)-neomenthol dehydrogenase-like isoform X2, structural maintenance of chromosomes protein 1, heat shock 70 kDa protein. Plant metabolism can be improved desirably by direct altering the miRNA-target interaction, using miRNA targeting mRNA that encodes for transcription factors [45]. This involve change in expression level of key genes involved in miRNA biosynthesis and processing and other pathways. Ideally silencing of one gene encoding protein involved in miRNA biosynthesis can hamper the synthesis of multiple miRNAs [46].

Secondary metabolites for example flavonoids, terpenoids, and alkaloids etc. are recognised for their participation in biotic stress. Their use in number of health care products is conventional. miRNAs are reported to regulate the various secondary metabolite biosynthesis like flavonoid biosynthesis, terpanoid biosynthesis, alkaloid biosynthesis. miRNAs directly targeted the genes coding for the pathway enzymes [47–50]. Leaf transcripts coding for (+)-neomenthol dehydrogenase-like isoform X2, Cytochrome P450 90B1 and furostanol glycoside 26-O-beta-glucosidase-like are tragted by cbo-miR38. This showed the role of plant specific miRNA in secondary metabolite pathways. Whereas initially in our previous study, we found number of known miRNAs targeting MVA and MEP pathway. So here we got a specific mark for secondary metabolite metabolism.

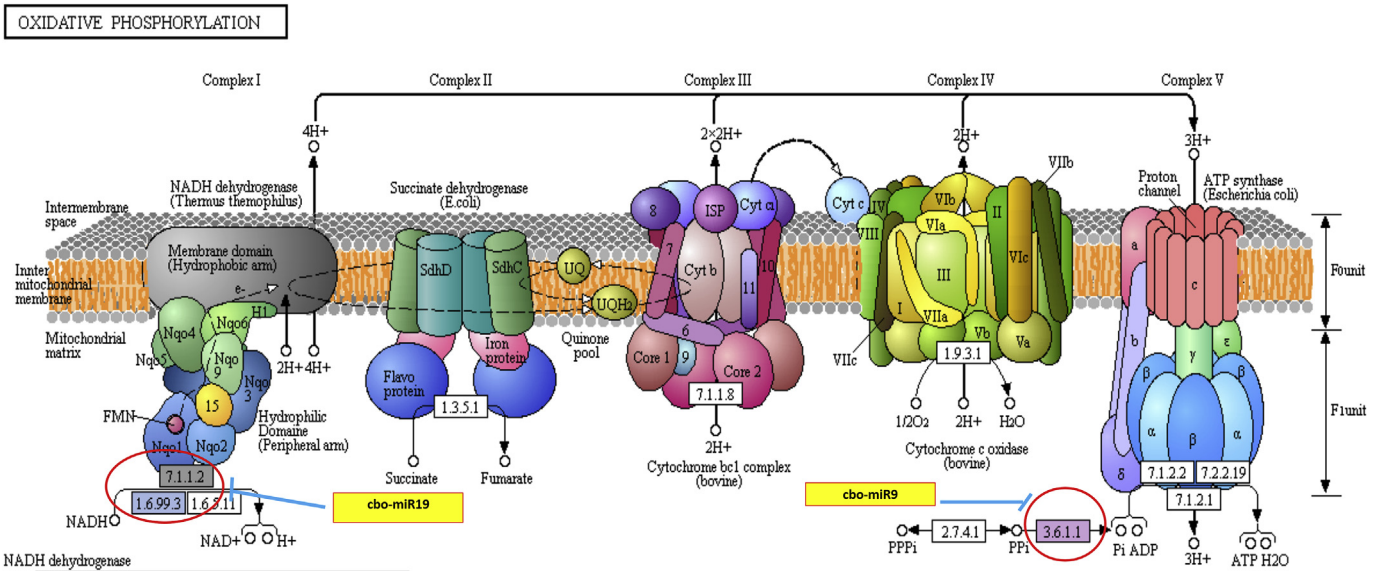

Fig. 5. Pictorial representation of novel miRNAs targeting oxidative phosphorylation in root tissue of *C. borivilianum* (ec:7.1.1.2 - reductase (H + -translocating), ec:1.6.99.3 – dehydrogenase, ec:3.6.1.1 – diphosphatase).

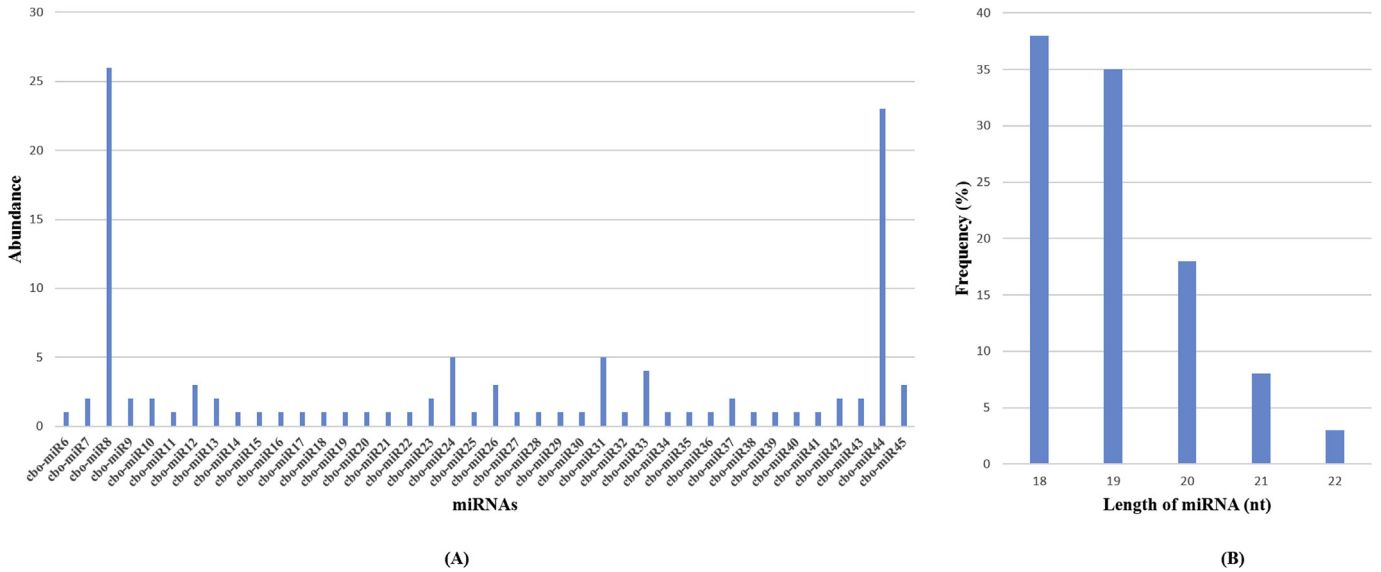

Fig. 6. (A) Abundance of novel miRNAs in *C. borivilianum*. (B) Frequency percentage of each length of novel miRNA in *C. borivilianum.*

3.2. Extensive array of novel miRNAs

However prior to this study, a pool of known and a few novel miRNAs was identified from *C. borivilianum* [17]. Prediction of novel miRNAs is difficult because they do not share sequence homology with known miRNAs, so no miRNA reference for their identification [51,52]. Even after about 2 decade of miRNAs discovery in plants, novel miRNAs identification process is still proceeding. It is well known that species-specific miRNAs supplement the function of conserved miRNAs in the regulation of specific regulatory pathways (Glazov et al., 2008). Total 40 new novel miRNAs were identified in our present study, further their target identification showed wide miRNAs regulation in *C. borivilianum.* Novel miRNA population varies in abundance like 35 novel miRNAs in blueberry [53], 35 in *Botrytis cinerea* [54], 38 in *Raphanus sativus* L. [55], 11 in Apple (Golden delicious) [56]. Novel miRNA length varies from 18 to 21 nt in *C. borivilianum.* novel miRNA of length 18 nt was most abundant in our population. Furthermore, length of potential miRNA precursor length varied from 65 to 99 nt. Minimum free energy (MFE) value ranged from −30.20 to 65.4 kcal/mol. For a stem-loop precursor, MFE should be less than −18 kcal/mol [57]. All these observation confirmed the existence of identified novel miRNAs in *C. borivilianum*.

4. Conclusion

A set of 40 novel miRNAs and along with their targets were searched in present study using degradome sequencing. The plant specific miRNA regulate multiple pathways that seems contrary to the fact that novel miRNAs are involved in only some specific pathways. Here, we found the role novel miRNAs in pathways like cellular functions, photosynthesis, secondary metabolism. cbo-miR24 and cbo-miR33 involved in photosynthesis was key fact observed in our study. Further experiments of up-regulation/down-regulation of identified miRNAs can in inclusive development of plant. This can ultimately help in overall crop yield. Current study will add on to the existing database of *C. borivilianum* and will further help in using miRNAs for improving plants' properties.

5. Methods and material

5.1. Plant material and RNA isolation

Vegetative buds from old *C. borivilianum* plants were selected to raise new plantlets. For optimal plant growth garden soil was mixed with peat moss (50%). Ideal condition for plant growth is 27 °C day/night temperature for a period of 16/8 h respectively. Young leaf tissue from the 2 month old plant, best suited for total RNA isolation was snap frozen using liquid nitrogen and stored at −80 °C.

Minor alterations were done in miRNeasy kit (Qiagen, Germany) protocol according to Ghawana et al., 2011 [58]. This relaxed the cumbersome of RNA isolation and enriched the total RNA with small RNA (including degraded product of small RNA) from a plant tissue with high phenolic content. This comprised fine grinding of 100 mg young leaf tissue using liquid nitrogen and homogenization with solution-I and solution-II. Further protocol for RNA isolation was followed according to manufacturer's instructions. On-column DNase digestion was performed to remove DNA contamination and nuclease free water was used RNA elution. Quantity of eluted RNA was measured using nanodrop spectrophotometer and quality was ensured by Agilent 2100 bioanalyzer system.

5.2. Small RNA sequencing and identification of novel miRNAs

Small RNA sequencing data from our previous study was processed further whose raw data is available in public domain under the SRA ID (SRP121214). In our previous study we found total 442 known miRNAs and 5 novel miRNAs from *C. borivilianum* [17]. Further to expand and refine the novel miRNA population, remaining unaligned reads were used for the prediction of more novel miRNAs by using reference of *Arabidopsis thaliana, Oryza sativa, Populus trichocarpa, Ricinus communis,* and *Vitis vinifera* genomes by miRDeep2 (version 2.0.0.7) tool [59]. As the genome of *C. borivilainum* is not known, wide variety of plant species were selected for reference that too included both monocot and dicots. This provided us to correlate the novel miRNAs of the test plant with a big miRNA pool. This further also helped in interlinking function regulation among selected species. The precise workflow is mentioned in Fig. 7. All predicted novel miRNAs were subjected to target prediction using degradome sequencing. Novel miRNAs, only with well defined functions were finally scrutinized. Selected novel miRNAs were named according to pre-defined criteria [24]. Details of each step is thoroughly explained in subsequent section.

5.3. Degradome sequencing and raw data processing

Extracted total RNA was sent to Genotypic Technology [P] Ltd., #2/13, Balaji Complex, 80 feet road, R.M.V. 2nd Stage, Bangalore-560094,

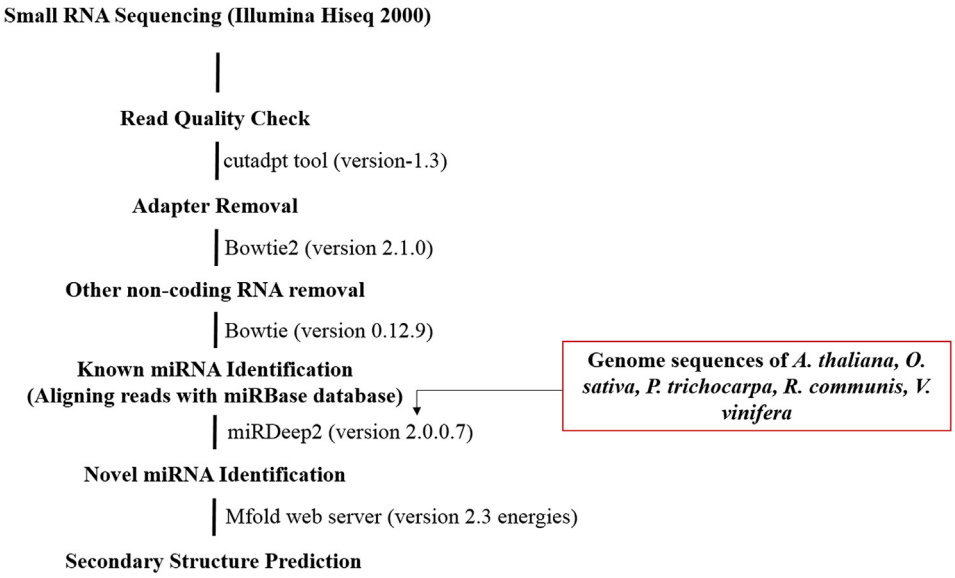

Fig. 7. Schematic representation of novel miRNA prediction.

INDIA, for degradome library preparation and sequencing. Total RNA (24 μg) was treated for poly (A) enrichment [Dynabeads® Oligo (dT)] and 5′-end DNA adapter ligation was done using T4 RNA ligase overnight at 16 °C. After removing unligated 5′-end adapters, first strand cDNA was synthesized using 5′-end adapters ligated mRNA. First strand cDNA synthesis included annealing of 3′ tailed random primer and superscript-III RT followed by removal of reagent traces by bead clean-up. 15 cycles of indexing PCR was done to enrich adapter-ligated fragments [Denaturation (95° C/3 min), cycling (95° C/30s, 55° C/30s, 72° C/45s) and 72° C/5mins]. This resulted into final sequencing library that was purified with JetSeq beads, followed by library quality control analysis. The quantification of sequencing library was done by Qubit fluorometer (Thermo Fisher Scientific, MA, USA) and its fragment size distribution was analysed on Agilent TapeStation. The sequencing was carried out by Illumina Nextseq Single-end sequencing (75 × 1) platform.

The raw data of length 75 bp was generated from Illumina platform and received in FASTQ format. srna-workbenchV3.0 ALPHA1 was used to trim 3′ adapter and performed length filtering (minimum length 16bp and maximum 40 bp) [60]. The low quality and contaminated reads were removed on the following criteria to obtain final clean reads, i) removal of reads with phred score less than 30 ii) reads devoid of 3′ adapters iii) reads lacking insert iv) accepted read length 16-40bp vi) reads aligning other ncRNAs (r, t, sn, and snoRNAs). A total of 14 million high quality and non-redundant reads were retained for analysis.

5.4. Prediction of novel miRNA targets

Tool Cleaveland4 was used for processing of degradome raw data. Here fasta reads were provided as input [19]. Filtered sequences from degradome data were aligned to the structural RNAs using the Oligomap short read aligner [61]. For every exact alignment with the sense strand of an mRNA, a 26-nt long 'query' mRNA subsequences was mined by extracting 13-nt long sequences from both upstream and downstream to the location of the 5′-end of the aligned degradome sequence. Needle program (EMBOSS) was used for aligning query sequences miRNA sequence data [62]. Alignments were then scored according to a previously described scheme developed for plant miRNA/target pairings [63]. Degradome sequences with 5′-end corresponding to the 10th nucleotide of miRNA as well as alignment score less than threshold were retained. To remove spurious results pipeline was re-ran using randomly shuffled miRNA sequences to minimize signal-to-noise ratios; shuffled sequences had di-nucleotide and tri-nucleotide compositions corresponding with those of the input transcriptome. Categorization of targets was done into the subsequent 5 categories (0, 1, 2, 3, or 4). The exact pipeline followed for the current analysis is well explained in Fig. 8.

On the basis of significant targets identified, we further filtered out the novel miRNAs. As it was assumed that if novel miRNAs could target transcript from leaf or root tissue, they must have actual availability in the plant. This provided us the list of novel miRNAs with high indemnity and confirmed their functionality.

5.5. Functional annotation and classification

Targets confirmed from degradome sequencing data analysis were subjected to Blast2GO 5 for Gene Ontology (GO) annotations. Annotation grouped all targets in following 3 cluster (i) Biological Process (BP), (ii) Molecular Function (MF), and (iii) Cellular Component (CC) [64]. Default parameters were used for Blast2GO. Finally, identified targets were assigned in biochemical pathways by Kyoto Encyclopedia of Genes and Genomes (KEGG) pathway analysis.

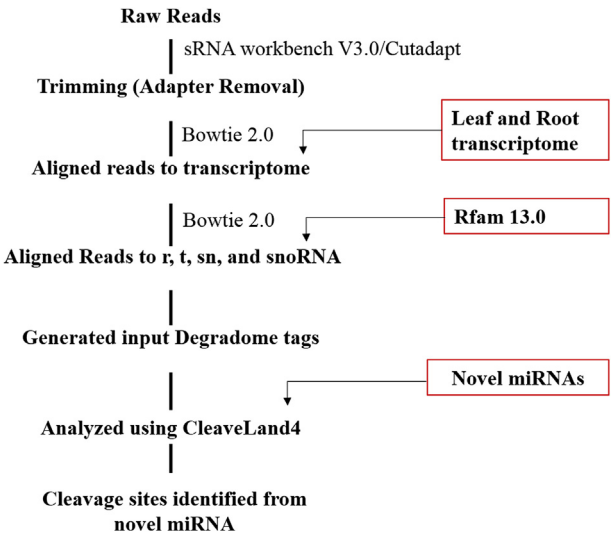

Fig. 8. Schematic representation of degradome analysis pipeline.

Authors' contribution

KS - Conceived the idea, designed the experiments and finalized the manuscript. MK - performed experiments, collected data, analysed results and wrote manuscript. NK and RK - performed bioinformatics analysis and helped in writing of manuscript.

Funding

Authors are grateful to CSIR, India for providing grant to carry out experiments.

Declaration of competing interest

The Authors declare that there are no competing interests.

Acknowledgements

Authors are grateful to CSIR, India for providing the funds to carry out research work. Monika Kajal is thankful to University Grant Commission, India for providing fellowship. Nishant Kaushal is thankful to UGC, India for BSR fellowship. Ravneet Kaur is thankful to DST for WOS-A fellowship.

Appendix A. Supplementary data

Supplementary data to this article can be found online at https://doi.org/10.1016/j.ncrna.2019.11.004.

References

[1] M. Thakur, S. Bhargava, V. Dixit, Immunomodulatory activity of chlorophytum borivilianum sant, F, Evidence-Based complementary and alternative medicine 4 (2007) 419–423.
[2] M. Mujeeb, S.A. Khan, M. Ali, A. Mall, A. Ahmad, Antidiabetic activity of the aqueous extract of Chlorophytum borivilianum L. in streptozotocin induced-hyperglycemic rats: a preliminary study, J. Pharm. Res. 2 (2009).
[3] M. Thakur, V. Dixit, Effect of some vajikaran herbs on pendiculation activities and in vitro sperm count in male, Sex. Disabil. 25 (2007) 203–207.
[4] M. Thakur, V. Dixit, Effect of Chlorophytum borivilianum on androgenic & sexual behavior of male rats, INDIAN DRUGS-BOMBAY 43 (2006) 300.
[5] W. IUCN, Draft) Guidelines for Recognising and Reporting Other Effective Area-Based Conservation Measures, IUCN, Switzerland, 2018 Version, 1.
[6] S. Kalra, B.L. Puniya, D. Kulshreshtha, S. Kumar, J. Kaur, S. Ramachandran, K. Singh, De novo transcriptome sequencing reveals important molecular networks and metabolic pathways of the plant, Chlorophytum borivilianum, PLoS One 8 (2013) e83336.
[7] S. Kumar, S. Kalra, S. Kumar, J. Kaur, K. Singh, Differentially expressed transcripts from leaf and root tissue of Chlorophytum borivilianum: a plant with high medicinal value, Gene 511 (2012) 79–87.
[8] S. Kalra, S. Kumar, N. Lakhanpal, J. Kaur, K. Singh, Characterization of squalene synthase gene from Chlorophytum borivilianum (Sant. and Fernand.), Mol. Biotechnol. 54 (2013) 944–953.
[9] S. Kumar, S. Kalra, B. Singh, A. Kumar, J. Kaur, K. Singh, RNA-Seq mediated root transcriptome analysis of Chlorophytum borivilianum for identification of genes involved in saponin biosynthesis, Funct. Integr. Genom. 16 (2016) 37–55.
[10] D.P. Bartel, MicroRNAs: target recognition and regulatory functions, Cell 136 (2009) 215–233.
[11] G. Meister, T. Tuschl, Mechanisms of gene silencing by double-stranded RNA, Nature 431 (2004) 343.
[12] S.-R. Liu, J.-J. Zhou, C.-G. Hu, C.-L. Wei, J.-Z. Zhang, MicroRNA-mediated gene silencing in plant defense and viral counter-defense, Front. Microbiol. 8 (2017) 1801.
[13] R.W. Carthew, E.J. Sontheimer, Origins and mechanisms of miRNAs and siRNAs, Cell 136 (2009) 642–655.
[14] J. Liu, M.A. Carmell, F.V. Rivas, C.G. Marsden, J.M. Thomson, J.-J. Song, S.M. Hammond, L. Joshua-Tor, G.J. Hannon, Argonaute 2 is the catalytic engine of mammalian RNAi, Science 305 (2004) 1437–1441.
[15] K. Rogers, X. Chen, Biogenesis, turnover, and mode of action of plant microRNAs, The Plant Cell 25 (2013) 2383–2399.
[16] J. Tang, C. Chu, MicroRNAs in crop improvement: fine-tuners for complex traits, Nature plants 3 (2017) 17077.
[17] M. Kajal, K. Singh, Small RNA profiling for identification of miRNAs involved in regulation of saponins biosynthesis in Chlorophytum borivilianum, BMC Plant Biol. 17 (2017) 265.
[18] C. Llave, Z. Xie, K.D. Kasschau, J.C. Carrington, Cleavage of Scarecrow-like mRNA targets directed by a class of Arabidopsis miRNA, Science 297 (2002) 2053–2056.
[19] C. Addo-Quaye, W. Miller, M.J. Axtell, CleaveLand: a pipeline for using degradome data to find cleaved small RNA targets, Bioinformatics 25 (2008) 130–131.
[20] M.A. German, M. Pillay, D.H. Jeong, A. Hetawal, S. Luo, P. Janardhanan, V. Kannan, L.A. Rymarquis, K. Nobuta, R. German, E. De Paoli, C. Lu, G. Schroth, B.C. Meyers, P.J. Green, Global identification of microRNA-target RNA pairs by parallel analysis of RNA ends, Nat. Biotechnol. 26 (2008).
[21] A. Adai, C. Johnson, S. Mlotshwa, S. Archer-Evans, V. Manocha, V. Vance, V. Sundaresan, Computational prediction of miRNAs in Arabidopsis thaliana, Genome Res. 15 (2005) 78–91.
[22] S. Caffarri, T. Tibiletti, R.C. Jennings, S. Santabarbara, A comparison between plant photosystem I and photosystem II architecture and functioning, Curr. Protein Pept. Sci. 15 (2014) 296–331.
[23] A. Makino, Photosynthesis, grain yield, and nitrogen utilization in rice and wheat, Plant Physiol. 155 (2011) 125–129.
[24] H. Budak, R. Bulut, M. Kantar, B. Alptekin, MicroRNA nomenclature and the need for a revised naming prescription, Briefings in functional genomics 15 (2015) 65–71.
[25] A. Sheriff, Karyomorphology of four diploid species of Chlorophytum, Nucleus 15 (1972) 39–45.
[26] V. Nair, Cytological studies in chlorophytum bruchae ansari, Curr. Sci. 43 (1974) 161.
[27] Z. Khanam, O. Singh, R. Singh, I.U.H. Bhat, Safed musli (Chlorophytum borivilianum): a review of its botany, ethnopharmacology and phytochemistry, J. Ethnopharmacol. 150 (2013) 421–441.
[28] S. Rohit, S. Nidhi, T.S. Gulab, S.S. Bhagwan, J. Pallavi, Conventional method for saponin extraction from Chlorophytum borivilianum Sant. et Fernand, Glob. J. Res. Med. Plants Indig. Med. 3 (2014) 33.
[29] R. Kaur, S. Arora, A. Thukral, Quantitative and qualitative analysis of saponins in different plant parts of Chlorophytum borivilianum, Int. J. Pharma Bio Sci. 6 (2015) 826–835.
[30] S.S. Giri, S.S. Sen, C. Chi, H.J. Kim, S. Yun, S.C. Park, V. Sukumaran, Chlorophytum borivilianum polysaccharide fraction provokes the immune function and disease resistance of Labeo rohita against Aeromonas hydrophila, Journal of immunology research (2015) 2015.
[31] N. Giribabu, K.E. Kumar, S.S. Rekha, S. Muniandy, N. Salleh, Chlorophytum borivilianum root extract maintains near normal blood glucose, insulin and lipid profile levels and prevents oxidative stress in the pancreas of streptozotocin-induced adult male diabetic rats, Int. J. Med. Sci. 11 (2014) 1172.
[32] G. Ji, P. Dwivedi, S. Sundaram, R. Prakash, Inhibitive effect of chlorophytum borivilianum root extract on mild steel corrosion in HCl and H2SO4 solutions, Ind. Eng. Chem. Res. 52 (2013) 10673–10681.
[33] L. Beauclair, A. Yu, N. Bouché, microRNA-directed cleavage and translational repression of the copper chaperone for superoxide dismutase mRNA in Arabidopsis, Plant J. 62 (2010) 454–462.
[34] M.R. Fabian, N. Sonenberg, W. Filipowicz, Regulation of mRNA translation and stability by microRNAs, Annu. Rev. Biochem. 79 (2010) 351–379.
[35] L. Wu, H. Zhou, Q. Zhang, J. Zhang, F. Ni, C. Liu, Y. Qi, DNA methylation mediated by a microRNA pathway, Mol. Cell 38 (2010) 465–475.
[36] B. Khraiwesh, M.A. Arif, G.I. Seumel, S. Ossowski, D. Weigel, R. Reski, W. Frank, Transcriptional control of gene expression by microRNAs, Cell 140 (2010) 111–122.
[37] A. Kozomara, S. Griffiths-Jones, miRBase: annotating high confidence microRNAs using deep sequencing data, Nucleic Acids Res. 42 (2013) D68–D73.
[38] D. Liu, R. Mewalal, R. Hu, G.A. Tuskan, X. Yang, New technologies accelerate the exploration of non-coding RNAs in horticultural plants, Horticulture research 4 (2017) 17031.
[39] X. Zhang, H. Zhao, S. Gao, W.-C. Wang, S. Katiyar-Agarwal, H.-D. Huang, N. Raikhel, H. Jin, Arabidopsis Argonaute 2 regulates innate immunity via miRNA393*-mediated silencing of a Golgi-localized SNARE gene, MEMB12, Mol. Cell 42 (2011) 356–366.
[40] W. Hu, T. Wang, E. Yue, S. Zheng, J.-H. Xu, Flexible microRNA arm selection in rice, Biochem. Biophys. Res. Commun. 447 (2014) 526–530.
[41] Y. Meng, X. Ma, D. Chen, P. Wu, M. Chen, MicroRNA-mediated signaling involved in plant root development, Biochem. Biophys. Res. Commun. 393 (2010) 345–349.
[42] A. De Luis, K. Markmann, V. Cognat, D.B. Holt, M. Charpentier, M. Parniske, J. Stougaard, O. Voinnet, Two microRNAs linked to nodule infection and nitrogen-fixing ability in the legume Lotus japonicus, Plant Physiol. 160 (2012) 2137–2154.
[43] S. Jayasena, A. Reynolds, A. Khvorova, RNA Interference, in, Google Patents, 2004.
[44] X. Chi, Q. Yang, X. Chen, J. Wang, L. Pan, M. Chen, Z. Yang, Y. He, X. Liang, S. Yu, Identification and characterization of microRNAs from peanut (Arachis hypogaea L.) by high-throughput sequencing, PLoS One 6 (2011) e27530.
[45] V.P. Bulgakov, T.V. Avramenko, New opportunities for the regulation of secondary metabolism in plants: focus on microRNAs, Biotechnol. Lett. 37 (2015) 1719–1727.
[46] G.J. Kettles, C. Drurey, H.j. Schoonbeek, A.J. Maule, S.A. Hogenhout, Resistance of Arabidopsis thaliana to the green peach aphid, Myzus persicae, involves camalexin and is regulated by microRNAs, New Phytol. 198 (2013) 1178–1190.
[47] S. Biswas, S. Hazra, S. Chattopadhyay, Identification of conserved miRNAs and their putative target genes in Podophyllum hexandrum (Himalayan Mayapple), Plant Gene 6 (2016) 82–89.
[48] M. Zhang, Y. Dong, L. Nie, M. Lu, C. Fu, L. Yu, High-throughput sequencing reveals miRNA effects on the primary and secondary production properties in long-term subcultured Taxus cells, Front. Plant Sci. 6 (2015) 604.
[49] R. Yang, Y. Zeng, X. Yi, L. Zhao, Y. Zhang, Small RNA deep sequencing reveals the important role of micro RNA s in the halophyte Halostachys caspica, Plant biotechnology journal 13 (2015) 395–408.
[50] J. Wu, D. Wang, Y. Liu, L. Wang, X. Qiao, S. Zhang, Identification of miRNAs

involved in pear fruit development and quality, BMC Genomics 15 (2014) 953.
[51] N. Mendes, A.T. Freitas, M.-F. Sagot, Current tools for the identification of miRNA genes and their targets, Nucleic Acids Res. 37 (2009) 2419–2433.
[52] D. Kleftogiannis, A. Korfiati, K. Theofilatos, S. Likothanassis, A. Tsakalidis, S. Mavroudi, Where we stand, where we are moving: surveying computational techniques for identifying miRNA genes and uncovering their regulatory role, J. Biomed. Inform. 46 (2013) 563–573.
[53] J. Yue, X. Lu, H. Zhang, J. Ge, X. Gao, Y. Liu, Identification of conserved and novel microRNAs in blueberry, Front. Plant Sci. 8 (2017) 1155.
[54] Y. Liang, Y. Guan, S. Wang, Y. Li, Z. Zhang, H. Li, Identification and characterization of known and novel microRNAs in strawberry fruits induced by Botrytis cinerea, Sci. Rep. 8 (2018) 10921.
[55] W. Zhang, Y. Xie, L. Xu, Y. Wang, X. Zhu, R. Wang, Y. Zhang, E.M. Muleke, L. Liu, Identification of microRNAs and their target genes explores miRNA-mediated regulatory network of cytoplasmic male sterility occurrence during anther development in radish (Raphanus sativus L.), Front. Plant Sci. 7 (2016) 1054.
[56] C. Ma, Y. Lu, S. Bai, W. Zhang, X. Duan, D. Meng, Z. Wang, A. Wang, Z. Zhou, T. Li, Cloning and characterization of miRNAs and their targets, including a novel miRNA-targeted NBS–LRR protein class gene in apple (Golden Delicious), Mol. Plant 7 (2014) 218–230.
[57] B.H. Zhang, X.P. Pan, Q.L. Wang, P.C. George, T.A. Anderson, Identification and characterization of new plant microRNAs using EST analysis, Cell Res. 15 (2005) 336.
[58] S. Ghawana, A. Paul, H. Kumar, A. Kumar, H. Singh, P.K. Bhardwaj, A. Rani, R.S. Singh, J. Raizada, K. Singh, An RNA isolation system for plant tissues rich in secondary metabolites, BMC Res. Notes 4 (2011) 85.
[59] M.R. Friedländer, W. Chen, C. Adamidi, J. Maaskola, R. Einspanier, S. Knespel, N. Rajewsky, Discovering microRNAs from deep sequencing data using miRDeep, Nat. Biotechnol. 26 (2008) 407.
[60] M.B. Stocks, S. Moxon, D. Mapleson, H.C. Woolfenden, I. Mohorianu, L. Folkes, F. Schwach, T. Dalmay, V. Moulton, The UEA sRNA workbench: a suite of tools for analysing and visualizing next generation sequencing microRNA and small RNA datasets, Bioinformatics 28 (2012) 2059–2061.
[61] P. Berninger, D. Gaidatzis, E. van Nimwegen, M. Zavolan, Computational analysis of small RNA cloning data, Methods 44 (2008) 13–21.
[62] P. Rice, I. Longden, A. Bleasby, EMBOSS: the European molecular biology open software suite, Trends Genet. 16 (2000) 276–277.
[63] E. Allen, Z. Xie, A.M. Gustafson, J.C. Carrington, microRNA-directed phasing during trans-acting siRNA biogenesis in plants, Cell 121 (2005) 207–221.
[64] A. Conesa, S. Götz, Blast2GO, A comprehensive suite for functional analysis in plant genomics, Int. J. Plant Genom. (2008) 2008.